NUMERICAL SOLUTION OF FLUID FLOW AND HEAT TRANSFER PROBLEMS WITH SURFACE RADIATION

S. Ahuja and K. Bhatia
Engineering Mechanics Research Corporation
Troy, Michigan

SUMMARY

This paper presents a numerical scheme, based on the finite element method, to solve strongly coupled fluid flow and heat transfer problems. The surface radiation effect for gray, diffuse and isothermal surfaces is considered. A procedure for obtaining the view factors between the radiating surfaces is discussed. The overall solution strategy is verified by comparing the available results with those obtained using this approach. An analysis of a thermosyphon is undertaken and the effect of considering the surface radiation is clearly explained.

INTRODUCTION

There are many engineering applications in which a coupled analysis of fluid flow and heat transfer is desired. Among a large list of such examples, a few important ones are design of heat exchangers, cooling of electronic components, climate control and underhood analyses in automobiles, performance of industrial furnaces, heat transfer analysis in confined cavities, and, cooling and heating of buildings, etc. The fluid flow analysis generally requires solution of conservation equations of mass and momentum. Several numerical approaches are available (refs. 1 to 4) under a variety of boundary conditions. In heat transfer studies usually energy conservation involving all three modes (namely, conduction, convection and radiation) is expected. However, until recently, conduction and convection heat transfer modes were accurately accounted for while approximations were made for including the radiation analysis (ref. 5). The high nonlinearity involved in the basic theory precluded from obtaining analytical solutions and a use of ordinary numerical methods for practical problems. The availability of cheaper computer resources has caught the attention of researchers wanting to include accurate radiation analyses in their studies. This is reflected in a collection of papers included in (ref. 6) published recently.

The aim of this paper is to present a numerical methodology for analyzing fluid flow and heat transfer problems (including all three modes). A brief account of numerical solution of Navier-Stokes and continuity equations using the finite element method is presented. The assumptions involving the heat transfer via radiation include non-participating fluids and gray, diffuse surfaces based on enclosure theory (ref. 8). Solution of strongly coupled (heat transfer and fluid flow) phenomenon with natural convection is demonstrated through a couple of examples. To benchmark the developed code, a comparison with the already reported results is made. This is followed by a discussion of results in an analysis involving a study of thermosyphon (ref. 9), a passive system used for cooling of electronic components.

GOVERNING EQUATIONS

In this section, the basic equations associated with the fluid flow and heat transfer are discussed. Generally, it suffices to consider the conservation of mass, momentum, and energy in the given domain of interest. In the presence of surface radiation, additional equation representing the conservation of radiative energy must also be considered. The effect of radiative fluxes on the relevant surfaces must be reflected in the overall energy balance. In summary, the following equations must be solved to conserve mass, momentum, energy, and radiative energy:

conservation of mass:

$$\frac{\partial u_k}{\partial x_k} = 0 \tag{1}$$

conservation of momentum:

$$\rho\left[\frac{\partial u_i}{\partial t} + u_k\frac{\partial u_i}{\partial x_k}\right] = -\frac{\partial p}{\partial x_i} + \frac{\partial}{\partial x_i}\left[\mu\left(\frac{\partial u_i}{\partial x_j} + \frac{\partial u_j}{\partial x_i}\right)\right] + \rho g_i\left[1 - \beta\,(T - T_\beta)\right] \tag{2}$$

conservation of energy:

$$\rho C\left[\frac{\partial T}{\partial t} + u_k\frac{\partial T}{\partial x_k}\right] = \frac{\partial}{\partial x_j}\left(k\frac{\partial T}{\partial x_j}\right) + Q \tag{3}$$

For explanation of the symbols employed, refer to the section titled Nomenclature. It should be noted that Equations (1) through (3) are used for incompressible fluid flow with Boussinesq approximations invoked to model the natural convection phenomenon.

conservation of surface radiative energy:

$$\sum_{j=1}^{N}\left(\frac{\delta_{ij}}{\varepsilon_j} - \frac{1-\varepsilon_j}{\varepsilon_j}F_{ij}\right)q_{rj} = \sum_{j=1}^{N}\left(\delta_{ij} - F_{ij}\right)\sigma T_j^4 - \left(1 - \sum_{j=1}^{N}F_{ij}\right)\sigma T_s^4 \tag{4}$$

In deriving Equation (4), it is assumed that the surfaces are gray, diffuse and isothermal (ref. 8). The view factors, F_{ij}, between surfaces i and j, appearing in Equation (4) must be computed when attempting the solution of this equation. In the next section, a discussion on view factor calculations is undertaken.

COMPUTATION OF VIEW FACTORS

In order to compute q_r's (in Equation (4)), view factors F_{ij}, between all radiating surfaces must be available. In this section, the physical meaning of viewfactor and its calculation will be discussed. For a better understanding, i,j in the above equation can be replaced with 1 and 2. Thus, view factor, F_{1-2}, between two arbitrary surfaces (see Figure 1), '1' and '2' is defined as a fraction of diffuse radiant energy leaving surface '1' that arrives at surface '2'. Mathematically,

$$F_{1-2} = \frac{1}{A_1} \int_{A1} \int_{A2} \frac{\text{Cos}\,\theta_1\, \text{Cos}\,\theta_2}{\pi\, r_{12}^2}\, dA_1\, dA_2 \qquad (5)$$

where A_1 and A_2 are the areas of surfaces 1 and 2, respectively, r_{12} is the distance between the two elemental areas dA_1 and dA_2, θ_1 is the angle between the position dependent normal vector $\vec{n}$ and the line connecting dA_1 and dA_2. Angle θ_2 is defined in a similar way. It must be noted that Cos θ_1 and Cos θ_2 must be positive in order for the surface dA_1 and dA_2 to 'see' each other. If either of the cosines has a negative value, the corresponding view factor, $F_{dA_1-dA_2}$ should be set to zero. Such cases, in which the inactive side of the radiating face acts as an obstructer, will be termed as 'self-obstruction' cases. Also, view factor F_{1-2} should be set to zero, if a third surface obstructs the view between surfaces 1 and 2.

In order to calculate view factors internally, the user must specify the radiation surfaces in terms of the finite element faces of a discretized domain. The user must also specify which of the two sides is a radiatively active side. These pieces of information can be supplied very easily via the already existing card in the NISA file of NISA/3D-FLUID. Each radiating face is taken as one radiation surface. View factors between the radiating surfaces are automatically generated by NISA/3D-FLUID taking into account self-obstruction and obstructions due to a third surface.

As can be assessed from the preceding discussion, computing view factors can result in usage of excessive computer time. To economize this computation, different techniques are used depending on whether the geometry being analyzed is 2D, 3D or axisymmetric. For example, double area integration method (ref. 8) is employed in comparison with contour integration method (ref. 8) when a 3D geometry, with radiation surfaces, is being analyzed. No special directives are required when computing view factors for axisymmetric geometries. NISA/3D-FLUID internally generates a complete 3D model (with the axis of symmetry as the X-axis [NISA/3D-FLUID]) to calculate the required view factors. Furthermore, for 2D problems, a completely different approach, called Hottel's crossed-string method (ref. 8) is employed for its computational efficiency and accuracy. Reference 8 provides more details for evaluating view factors for interested readers.

FE FORMULATION & SOLUTION PROCEDURE

The partial differential equations (Equations 1 through 3) and the radiative balance equation (Equation 4) are to be solved simultaneously to account for the fluid flow and heat transfer analyses in a given domain with specified boundary conditions. The convective terms appearing in Equations (2) and (3), simultaneous

solution of Equations (3) and (4), and arbitrary geometries encountered in most practical problems would require numerical tools for obtaining solution to coupled Equations 1 through 4. The Galerkin method in conjunction with the finite element method (ref. 8) form the basis of discretizing Equations 1 through 3. The penalty approach (ref. 3) is employed to eliminate the pressure from Equation (2) making use of Equation (1). For further details, refer to (refs. 3 and 10). The discretized form of Equations (2) and (3) can be written in matrix form as follows

$$[K]\{X\} = \{f\} \tag{6}$$

where Kij is the "stiffness" matrix, consisting of contributions from acceleration. diffusion and pressure gradient terms of Equation (2) and acceleration and diffusion terms of Equation (3). Xj represent [U, V, W] for momentum equations and [T] in the case of energy equation. The vector fj is discussed more at length as this contains coupling terms in Equations (2), (3), and (4). For example, the vector {f} for the momentum equations is

$$-\int_{\Omega} N^I \rho g_i \beta (T - T\beta)\, d\Omega + \int_{\Gamma} N^I (-P\delta_{ij} + \tau_{ij})\, n_j\, d\Gamma \tag{7}$$

Equation (7) indicates the influence of temperature distribution on the momentum equations while convective terms (included in Kij for Equation (3)) represent a dependence of the temperature field on the velocity distribution.

Furthermore fj for the energy equation consists of the following term:

$$f_j = \int_{\Omega} N^I Q\, d\Omega + \int_{\Gamma} N^I q\, d\Gamma \tag{8}$$

where

$$q = q_a + q_c + q_r \tag{9}$$

In the above equality, q_a, q_c, and q_r refer to the applied heat flux, effect due to convection boundary conditions, and that due to radiation on the boundary , respectively. The gray-body radiative effects can be considered via q_r which is evaluated using Equation (4) for a "known" temperature distribution. It is thus evident that Equations (3) and (4) are coupled via q_r and T. Far a complete enclosure. Equation (4) can be represented in the matrix as

$$[R]\{q_r\} = [S]\{T\} \tag{10}$$

where

$$R_{ij} = \sum_{j=1}^{N} \left(\frac{\delta_{ij}}{\varepsilon_j} - \frac{1-\varepsilon_j}{\varepsilon_j} F_{ij} \right) \tag{11}$$

and

$$S_{ij} = \sum_{j=1}^{N} \left(\delta_{ij} - F_{ij} \right) \sigma T_j^3 \tag{12}$$

Ideally Equations (6) for momentum and energy equations together with the radiative balance Equation (10) must be solved simultaneously. For practical reasons (computer memory and time, and nonlinearity in Equations (6) and (10)), a sequential approach is undertaken to solve these algebraic equations. Depending on the nature of coupling (strong for flows with free convective effects and weak for flows with forced convective effects), momentum, energy, and radiative balance equations are solved. For more details, refer to (ref. 10). It has been observed that q_r (and hence T) solution may not converge or may do so slowly. An under relaxation of q_r leads to its stabilization. This is achieved as follows:

$$q_{r_\bullet}^{i+1} = \alpha\, q_r^{i+1} + (1-\alpha)\, q_{r_\bullet}^{i} \tag{13}$$

where α is a user-defined relaxation factor. During a calculation sequence convergence checks are performed for velocity, temperature and surface flux, q_r, distributions by evaluating the L_2 norms. The sequential calculations are performed until the L_2 norms of all the nodal variables and surface radiation fluxes fall below a user-defined tolerance.

Special Cases:

There are a few special cases which require a slight modification to the above methodology for including the gray surface radiative effects in the heat transfer analysis. These are as follows:

a) Domain with plane(s) of symmetry
b) Exchange of radiative flux through "windows" in the domain
c) Exchange of radiative flux between the domain and surroundings
d) Radiative surfaces with no thickness.

The details of these modifications are presented in (ref. 10).

ILLUSTRATIONS

The aim of the present paper is to discuss an efficient solution strategy that must be undertaken to solve coupled fluid flow and heat transfer problems in the presence of radiative energy exchange between gray surfaces in a domain of interest with specified boundary conditions. In the previous sections, the pertinent differential equations and their respective discretized forms (using the finite element method) are discussed. In this section, a discussion of the results obtained with the outlined procedure for a couple of problems is undertaken.

Example 1: Natural Convection with and without Surface Radiative Effects in a Cavity.

The validation of the developed procedure is established by solving a problem studied by Behnia et al. (ref. 11). The fluid flow due to natural convective effects in a square cavity with radiating surfaces is considered. Figure 2 shows this cavity of a characteristic dimension, L and the specified boundary conditions. The top and bottom walls are adiabatic. The left wall is maintained at a uniform hot temperature, T_h. The right wall has convective and/or radiative boundary condition. The convective heat transfer coefficient is h. The temperature of the surroundings and the ambient temperature are taken to be T_∞. All the internal surfaces of the cavity have an emissivity of 0.9 and the fluid in the cavity is air. The cavity size, L, can be chosen to get a Rayleigh number of $3x10^5$. Table 1 shows a summary of conditions under which each case is analyzed with an aim of obtaining steady state temperature and fluid flow distributions in the cavity. Due to the presence of natural convective effects, strong coupling between the fluid flow and temperature fields is expected. The cavity is discretized into a graded mesh of 44 x 36 linear quadrilateral elements. The steady state algorithm of the code is invoked. Table 2 shows the relaxation parameters employed for each of the run detailed in Table 1 and the corresponding numbers of iterations required to obtain converged solutions.

Figure 3 shows the isotherms obtained for the cases denoted as R300, EC300, and REC300. A comparison of isotherms for these cases clearly indicates the effect of surface radiation on the adiabatic walls (top and bottom), the isotherms are no longer normal to these walls. Figure 4 shows the streamlines for the cases R300, EC300, and REC300 respectively. Table 3 shows a comparison of the maximum value of stream functions obtained for these runs with those listed in Behnia et al (ref. 11). A good quantitative agreement between the results is evident. Figure 5 shows the horizontal velocity along the vertical center line for these cases. The velocity profiles shown in the figure compare well with those in Figure 7 of ref. 11.

Example 2: Analysis of a Planar Thermosyphon.

In this example, the fluid flow and temperature distributions are studied in a thermosyphon including the surface radiative effects. A thermosyphon is a device used for cooling of electronic components, heat removal systems for nuclear reactors, and having applications in solar systems (ref. 9). Since thermosyphons involve no blowing or pumping of fluids, they are less expensive and more durable (termed as passive systems) as these do not require external signals for operation. A schematic of planar thermosyphon and the assigned boundary conditions is shown in Figure 6. An analysis of fluid flow and heat transfer in a thermosyphon is presented in (ref. 9) without the surface radiation effects. These effects have been included

in the study here. All the walls are black and are considered to be radiating. By observing the radiation surfaces in Figure 6, it is evident that all the surfaces cannot "see" each other. In other words, the view factor computation, in the presence of third surface obstructions, is invoked. These computations are more complex and handled efficiently in NISA/3D-FLUID (ref. 10).

First, the results are presented for the case in which only the convective effects (due to natural convection) are considered. The same analysis is performed in (ref. 9), in which the effects of varying the Rayleigh no. and a ratio of thermal conductivities of solid to fluid are considered. Therefore for the sake of comparison, results are presented for a Rayleigh no. of 10^4 and a ratio of thermal conductivities of 1 (see (ref. 9) for more details). Figure 7 shows the stream function distribution for this case and the corresponding isotherms are shown in Figure 8. A good agreement between these results and those presented in (ref. 9) is observed.

Now, the surface radiation effects due to the surfaces shown in Figure 6 is considered. The results for this case are not presented in (ref. 9). Figures 9 and 10 show distributions of stream functions and isotherms. A comparison of isotherms shown in Figures 8 and 10 indicate a considerable difference in their distributions. A further comparison of the velocity distributions, Figure 11, at "inlet" and "outlet" of the thermosyphon show marked differences. The difference in these velocity distributions amounts to a difference of 25% in flow rate. This analysis clearly indicates that if the surface radiation heat transfer is not accounted for, inaccurate distributions of temperatures and velocities may result.

CONCLUSIONS

A numerical scheme based on the finite element method is presented for solving coupled fluid flow and heat transfer problems in the presence of surface radiation. A sequential solution of momentum, energy and, radiative energy equations is considered for efficient computer memory management and disk usage. The computed results validated the numerical procedure adopted for an analysis of coupled fluid flow and heat transfer phenomena. The results presented compared well with those reported in literature. It is shown via the results discussed in this paper that the surface radiative effects must be considered for a complete heat transfer analysis. More research is underway to extend this work to consider non-gray surfaces and eventually participating fluids.

ACKNOWLEDGMENT

The authors are thankful to Jennie Kopacki for typing the manuscript.

NOMENCLATURE

C	=	Specific Heat	q	=	Heat Flux
g	=	Gravity Force	r	=	Spatial Coordinate
k	=	Thermal Conductivity	F	=	View Factor
p	=	Pressure	t	=	Time

Q	=	Volumetric Source	α, γ, φ	=	Relaxation Parameters
R	=	Radiation Matrix, LHS	ρ	=	Density
S	=	Radiation Matrix, RHS	β	=	Coefficient of Volume Expansion
T	=	Temperature	ε	=	Surface Emissivity
u	=	Velocity	δ	=	Kronecker Delta
F	=	Forcing Function	σ	=	Stefan-Boltzmamn Constant
X	=	Generalized Vector Nodal Unknown	Ω	=	Domain
N	=	Shape Functions	Γ	=	Boundary of the Domain
ψ	=	Stream Function	τ	=	Fluid Stress

Subscripts

β	=	Reference Temperature	r	=	Radiative
j	=	Spatial Index, Surface No.	i	=	Spatial Index, Surface No.
a	=	Applied Externally	s	=	Surroundings
c	=	Convective			

Superscripts

I	=	Nodal Index	i	=	Iteration No.

REFERENCES

1. Raithby, G.D.; and Schneider, G.E.: Numerical Solution of Problems in Incompressible Fluid Flow, Treatment of the Velocity -Pressure Coupling, Num. Heat Transfer, 1979, vol. 2, pp. 417-440.
2. Patankar, S.V.: A Calculation Procedure for Two Dimensional Elliptic Situations, Num. Heat Transfer, vol. 14, 1985, pp. 409-425.
3. Reddy, J.N.: Penalty Function Methods in the Finite Element Analysis of Fluid Flow, Int. J. Num. Methods in Fluids, vol. 2, 1982, pp. 151-171.
4. Hughes, T.J.R.; Taylor, R.L.; and Levy, J.F.: A Finite Element Method for Incompressible Viscous Flows, Proceedings of the 2nd Int-Symposium on Finite Element Methods in Fluid Flow Problems, Italy, 1976.
5. Ozisik, N.M.: Radiative Transfer, Wiley, New York, 1973.
6. Thynell, S.T. et al. (Editors), Developments in Radiative Heat Transfer, HTD-vol.203, ASME, 1993.
8. Siegel, R.; and Howell, J.R.: Thermal Radiation Heat Transfer, McGraw - Hill Book Company, New York, 1981.
7. Zienkiewicz, O.C.: The Finite Element Method, McGraw-Hill Book Company, New York, 1981.
9. Clarkson, R.; and Phillips, G.: A Parametric Study of Heat Transfer within a Planar Thermosyphon. HTD-vol. 237, ASME, 1993, pp. 9-19.
10. User's Manual, NISA/3D-FLUID, 1994.
11. Behnia, M.; J.A.; and de Vahl Davis, G.: Combined Radiation and Natural Convection in a Rectangular Cavity with Transparent Wall and Containing a Non-Participating Fluid, Int. J. Num. Meth-Fluids, vol. 10, 1990, pp. 305-325.

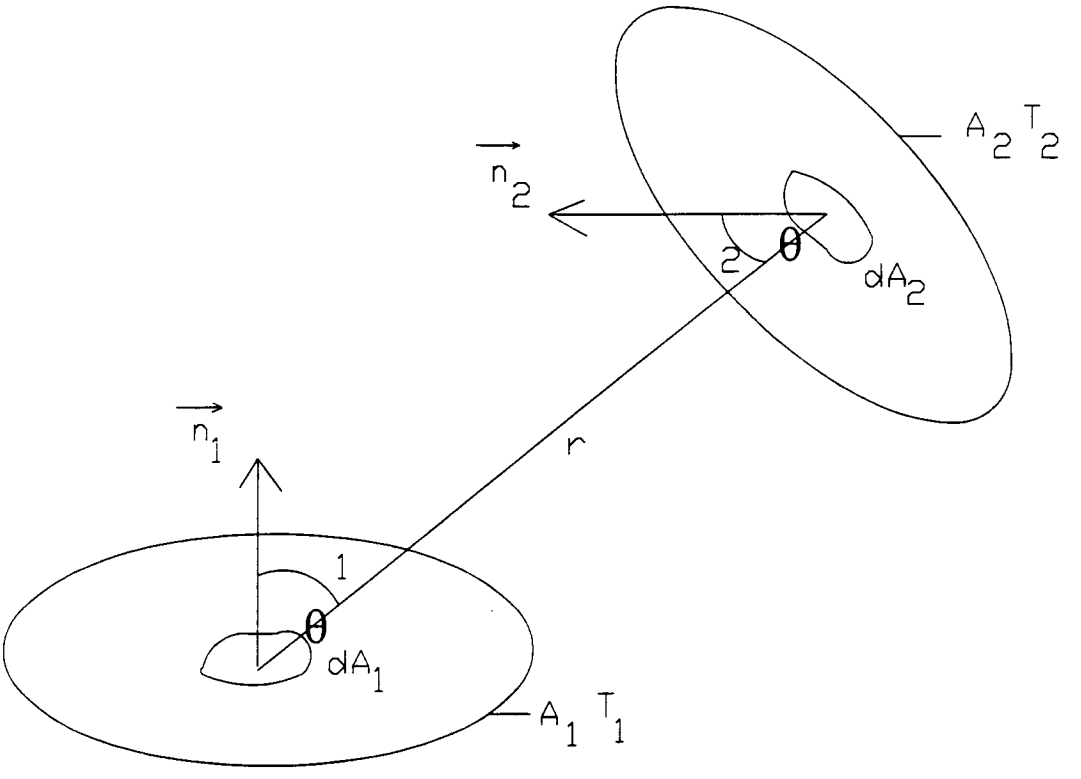

Figure 1 Definition of Terms Used in View Factor Calculations

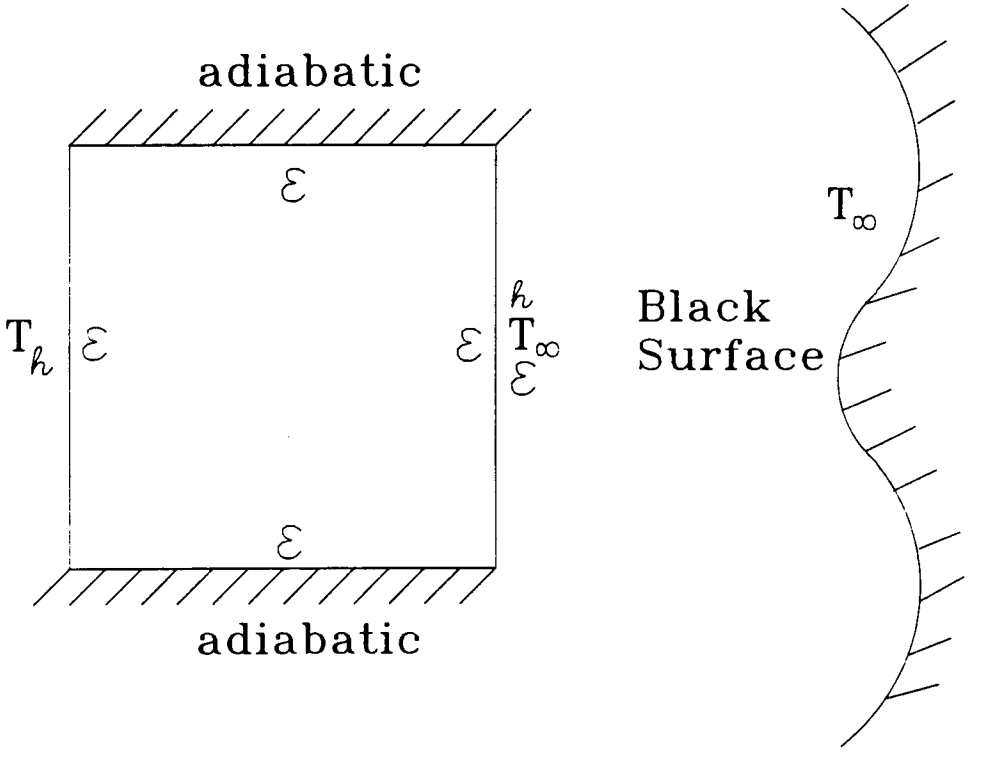

Figure 2 Schematic Diagram for Example 1

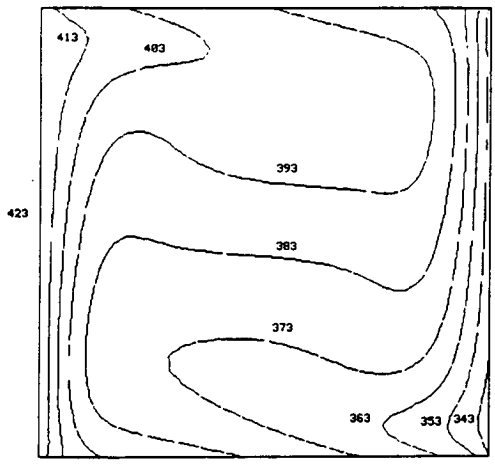

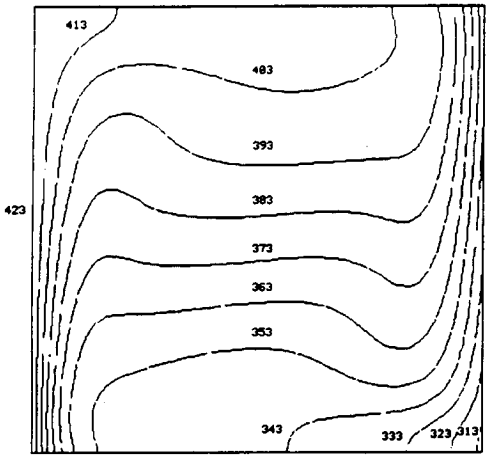

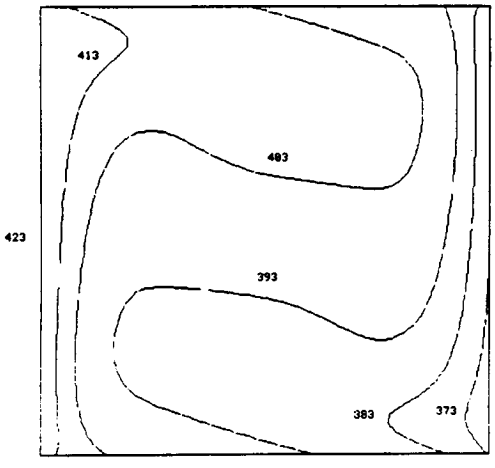

Figure 3 Isotherms for Runs REC300, EC300 and R300

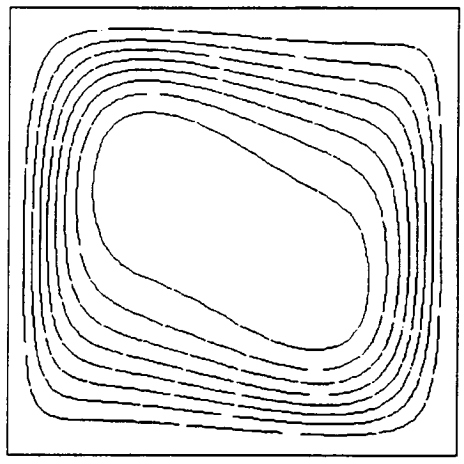

REC300

min.: -3.782×10^{-4} m^2/s max.: 0 m^2/s

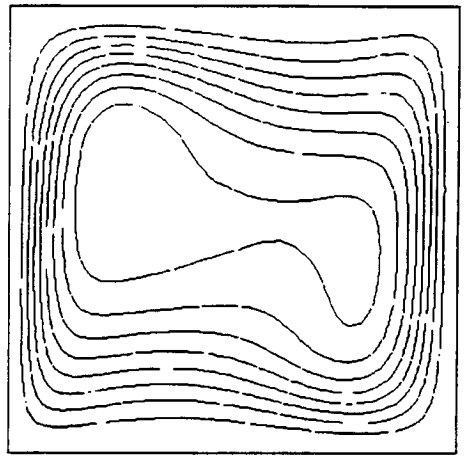

EC300

min.: -3.217×10^{-4} m^2/s max.: 0 m^2/s

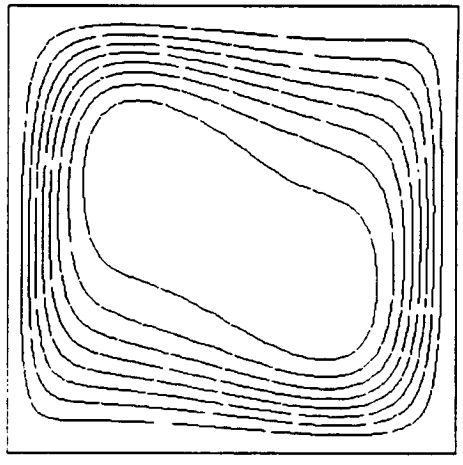

R300

min.: -3.444×10^{-4} m^2/s max.: 0 m^2/s

Figure 4 Streamlines for Runs REC3000, EC3000 and R300

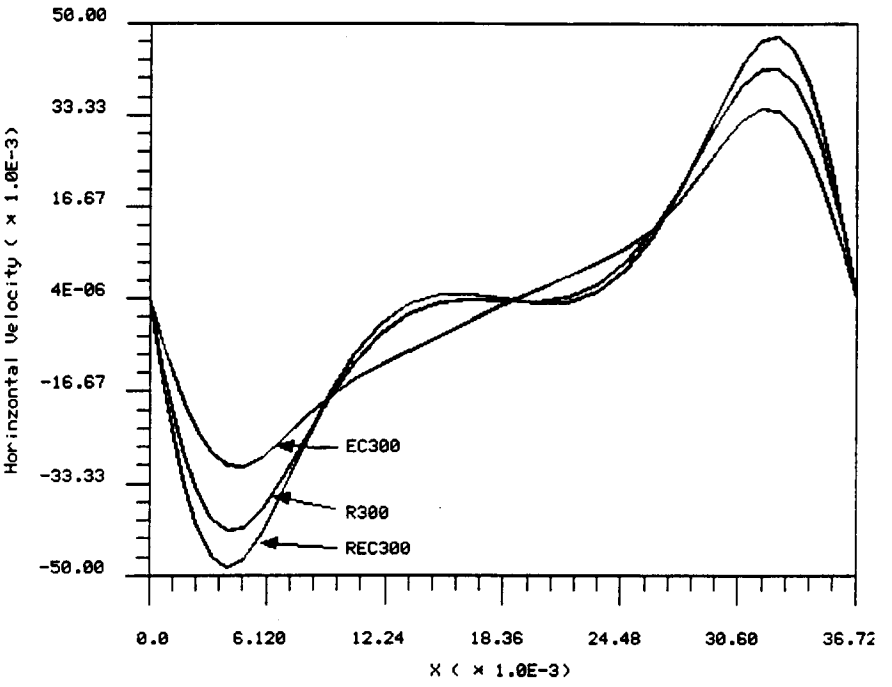

Figure 5 Horizontal Velocity Distributiuon Along the Vertical Centerline for Runs REC300, EC300 and RC300

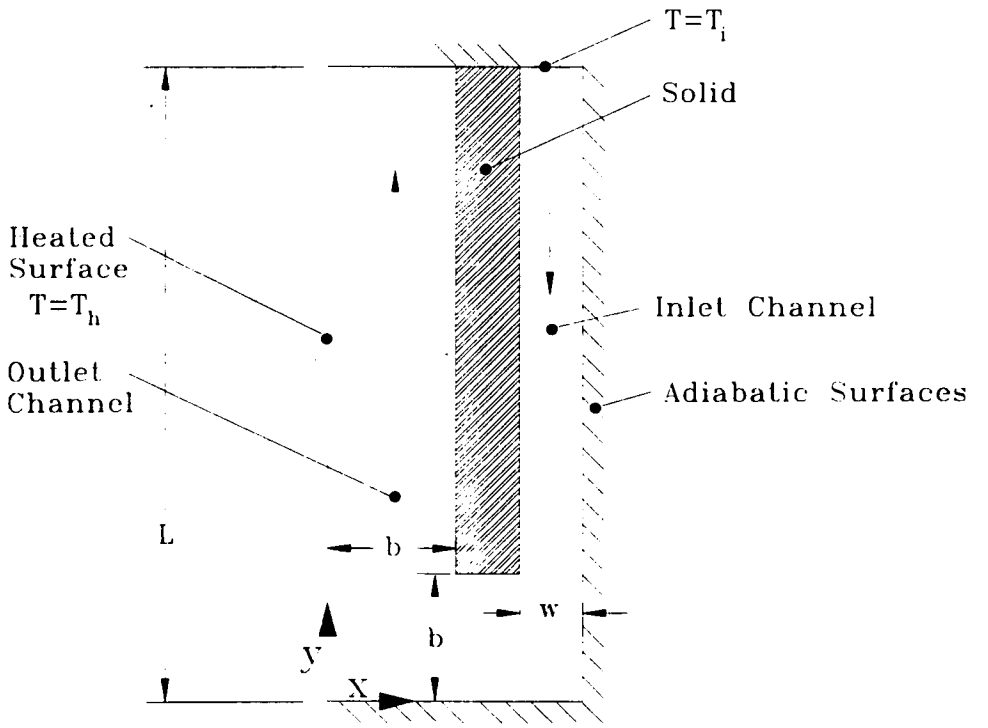

Figure 6 Schematic Diagram for Example 2 (Thermosyphon)

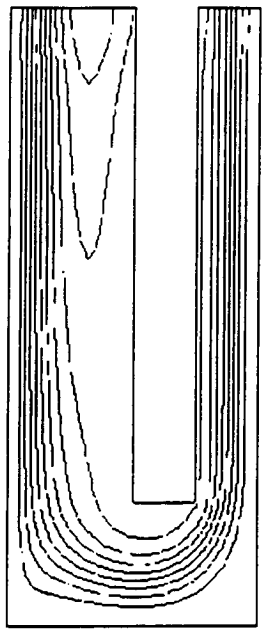

Figure 7 Streamlines for Thermosyphon (without Radiation)

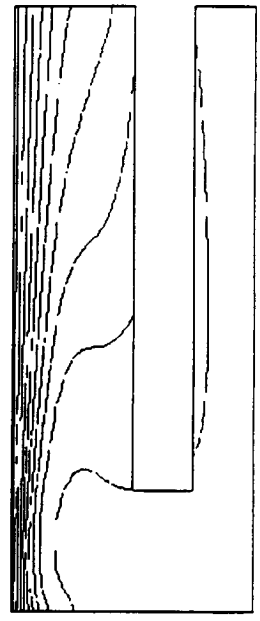

Figure 8 Isotherms for Thermosyphon (without Radiation)

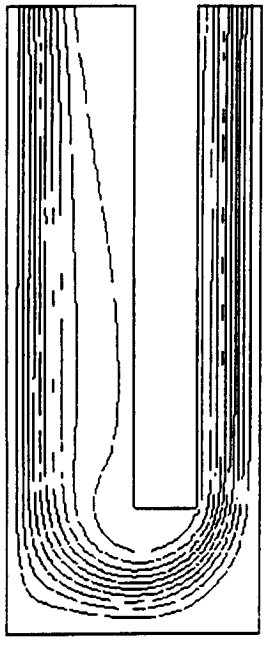

Figure 9 Streamlines for Thermosyphon (with Radiation)

Figure 10 Isotherms for Thermosyphon (with Radiation)

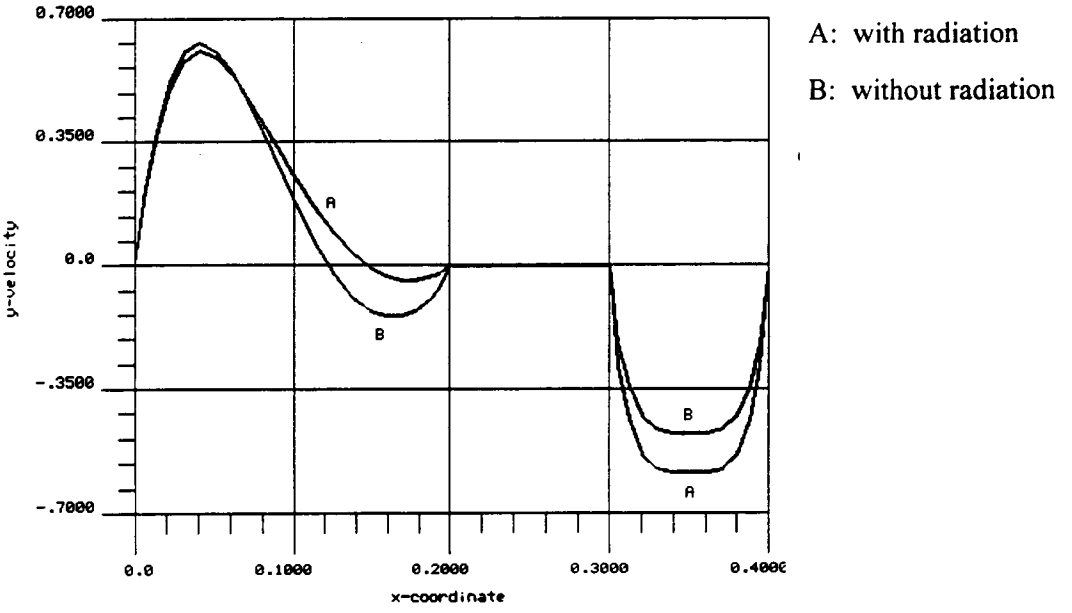

Figure 11 Inlet and Outlet Velocity Distributions for Thermosyphon

Table 1 Summary of Three Different Runs

Run	Ra	B.C. on the right wall	Surface Radiation
REC300	300,000	Convective + radiative	included
EC300	300,000	Convective	not included
R300	300,000	Radiative	included

$$Ra = Gr\,Pr = \frac{\rho^2 g \beta (T_h - T_\infty) L^3}{\mu^2} \cdot \frac{Cp\,\mu}{k}$$

Table 2 Relaxation Parameters and Number of Iterations

Run	Relaxation Parameter			No. of iterations
	Velocity α	Temperature γ	Radiative heat flux Φ	
REC300	0.04	1.0	0.1	64
EC300	0.04	1.0	0.1	40
R300	0.04	1.0	0.1	68

Table 3 Values of $|\Psi'|_{max}$ for Different Runs

Run	$\|\Psi'\|max = \frac{\|\Psi\|_{max}}{\alpha}$, $\alpha = \frac{k}{\rho C_p}$	
	Behnia et al. (ref. 11)	NISA/3D-FLUID (ref. 10)
REC300	13.04	12.94
EC300	10.93	11.01
R300	11.93	11.79